Journal of Alloys and Compounds 509 (2011) 4676–4681

Contents lists available at ScienceDirect

Journal of Alloys and Compounds

journal homepage: www.elsevier.com/locate/jallcom

Crystallographic relationship of orthorhombic φ-$Al_5Mg_{11}Zn_4$ phase to icosahedral quasicrystalline phase

Alok Singh*, J.M. Rosalie, H. Somekawa, T. Mukai

Lightweight Alloys Group, Structural Metals Center, National Institute for Materials Science, 1-2-1 Sengen, Tsukuba 305-0047, Japan

ARTICLE INFO

Article history:
Received 25 November 2010
Received in revised form 19 January 2011
Accepted 20 January 2011
Available online 3 February 2011

Keywords:
Quasicrystals
Crystal structure
Transmission electron microscopy (TEM)
Intermetallics

ABSTRACT

The orthorhombic φ-$Al_5Mg_{11}Zn_4$ phase is known to be related to quasicrystalline phases, but the exact relationship has not been shown yet. In this study, the relationship of this phase to the icosahedral quasicrystalline phase is explored through analysis of the electron diffraction patterns. It is shown that icosahedral coordinations in three orientations occur in the unit cell – one with three mutually perpendicular twofold axes along ⟨1 0 0⟩ of the unit cell, and two with a twofold axis along [1 0 0] and a fivefold along [0 0 1]. In this, this phase is similar to aluminum and zinc based hexagonal phases which are related to quasicrystals.

1. Introduction

Magnesium alloys are becoming increasingly important for structural applications for energy efficient vehicles which impact less on the environment. Common alloying elements in magnesium alloys are aluminum and zinc, forming AZ and ZK alloy series [1]. The AZ alloys are basically Mg–Al binary with equilibrium γ-$Mg_{17}Al_{12}$ phase as the strengthening phase.

In the Mg–Al–Zn ternary alloy system occur two ternary phases, one of which is the well known Bergman phase $Mg_{32}(Al, Zn)_{49}$, Im3 with lattice parameter a = 1.422 nm [2]. The structure of this phase is described as clusters at corners and body centered sites. These clusters consist of layers with icosahedral and dodecahedral coordination of atoms [2]. Thus this phase is closely related to the quasicrystalline icosahedral phase. It is a model structure for a class of crystals closely related to quasicrystalline phases known as rational approximants. Rational approximant structures are crystalline structures but with quasicrystal motifs (i.e., occurrence of icosahedral clusters in the structure). This relationship is brought out in the intensity modulation of spots in electron diffraction patterns. The diffraction spots in these phases are arranged periodically, but some of the spots are intense and make the diffraction pattern resemble quasicrystal diffraction patterns. The structure of these phases can be generated by projection from higher dimensions by approximating the Golden mean τ with a ratio of successive numbers (F_{n+1}/F_n) in the Fibonacci series [3–5]. Cubic phases α-AlMnSi [6] and $Mg_{32}(Zn, Al)_{48}$ [2] are well known examples of approximants to the icosahedral quasicrystal and are described as $F_{n+1}/F_n = 1/1$ [7–10]. The rational approximant structures of the icosahedral quasicrystal can be cubic, orthorhombic or rhombohedral, i.e., a subset of the symmetry of the icosahedral phase. Each unit cell dimension of a rational approximant phase is given as [11] as

$$\frac{2(p_i + q_i\tau)a_R}{\sqrt{\tau+2}}, \quad i = 1-3 \tag{1}$$

where a_R = quasilattice parameter, is the length of sides of the prolate and oblate rhombohedron defining the tiling in the physical space. The ideal quasicrystalline structure is obtained when

$$\frac{q_1}{p_1} = \frac{q_2}{p_2} = \frac{q_3}{p_3} = \tau$$

It has been demonstrated that on rapid solidification an alloy with a composition of the Bergman phase forms into an icosahedral phase [12,13]. Icosahedral phase is also formed on conventional solidification in alloys such as ZA84 [14].

The other ternary phase in the Mg–Al–Zn system, φ-$Al_5Mg_{11}Zn_4$ phase, is reported to have a space group Pbcm and lattice parameters a = 0.90 nm, b = 1.70 nm and c = 1.97 nm [15,16]. From the appearance of the electron diffraction patterns, a relationship to the icosahedral phase has been pointed out [15]. A structure of the φ-phase has been proposed, in which $Mg_5(Zn, Al)_{12}$ Friauf polyhedron is the main structural unit [16]. In alloys such as ZA84, the metastable icosahedral phase transforms directly to the φ-phase (with a change in the composition), which is the stable phase for the composition of the alloy [14]. In this study, the relationship of

* Corresponding author. Tel.: +81 29 859 2346; fax: +81 29 859 2301.
E-mail address: alok.singh@nims.go.jp (A. Singh).

0925-8388/$ – see front matter © 2011 Elsevier B.V. All rights reserved.
doi:10.1016/j.jallcom.2011.01.153

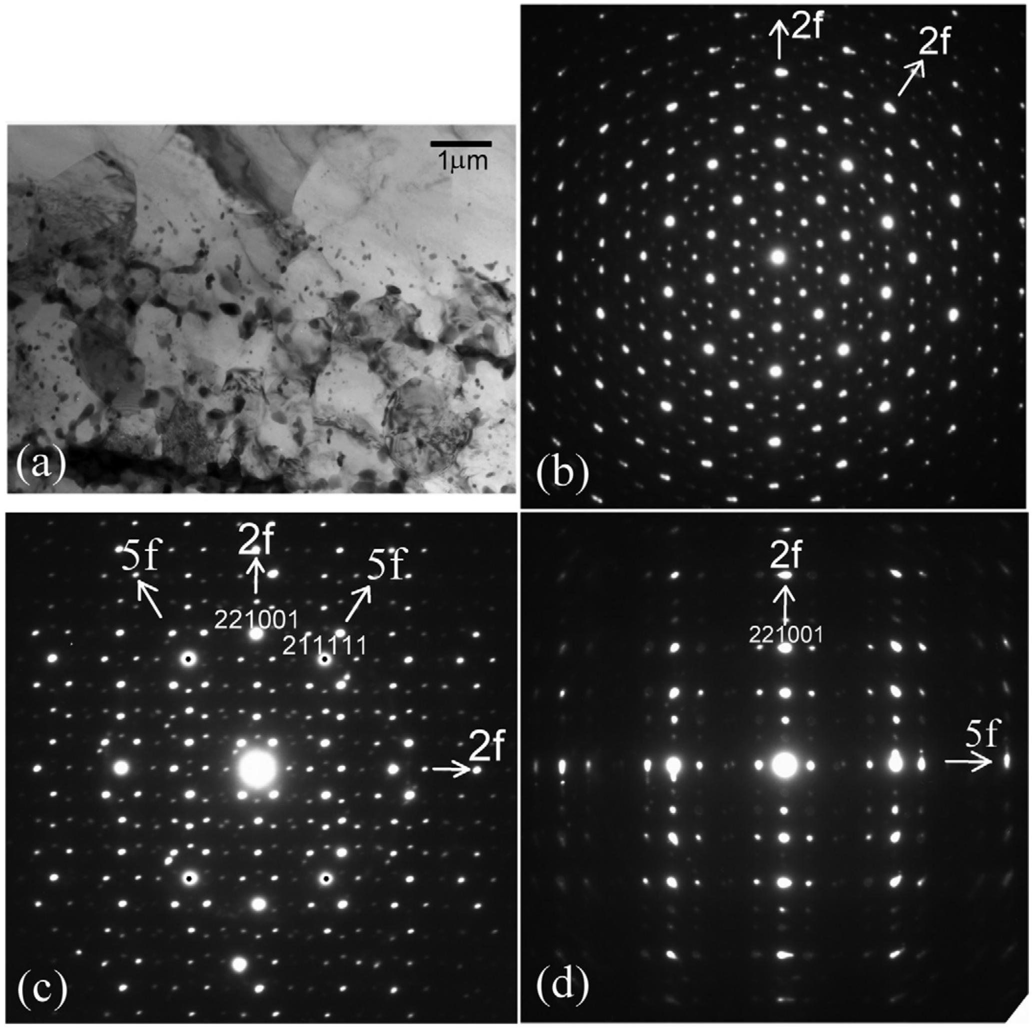

Fig. 1. (a) A bright field micrograph from the ZA84 alloy cast and extruded at 300 °C. A mixture of icosahedral phase and orthorhombic φ-phase occurred in the matrix. (b) A fivefold diffraction pattern from the icosahedral phase. Two of the five twofold reciprocal vectors are marked by arrows. (c) An icosahedral twofold diffraction pattern. Twofold and fivefold vectors are indicated. (d) An icosahedral ⟨τ 1 0⟩ diffraction pattern.

the φ-phase to the icosahedral phase is analyzed through electron diffraction patterns.

2. Experimental procedure

A ZA84 alloy (8 wt% Zn and 4 wt% Al) was prepared by melting under the cover of an inert gas and cast in a metallic mold. It was then extruded at 300 °C. Samples for observations in transmission electron microscope (TEM) were cut from the extruded bar by a low speed diamond saw, mechanically thinned and then polished by a precision ion mill. The TEM observations were performed on a JEOL 2000FX-II microscope.

3. Results

The solidified alloy contained an icosahedral phase at the grain boundaries. After extrusion, a mixture of the icosahedral phase and the φ-phase occurred. This is shown in the bright field micrograph of Fig. 1a. Fig. 1b shows a fivefold diffraction pattern from the icosahedral phase. The fivefold zone axis consists of five twofold reciprocal vectors, directions of two of which are marked by arrows in this diffraction pattern. Fig. 1c is a twofold diffraction pattern from the icosahedral phase. It contains two twofold reciprocal vectors and two fivefold reciprocal vectors. Along fivefold and twofold reciprocal vectors in an icosahedral phase occur the highest intensity spots {2 1 1 1 1 1} and {2 2 1 0 0 1}, respectively (using the indexing scheme of Elser [17]). The four {2 1 1 1 1 1} spots in this twofold diffraction pattern, marked by dots, make a rectangle called the Golden rectangle, because the ratio of the length of its sides is the Golden mean $\tau = (1+5)^{1/2}/2 = 1.618034\ldots$ The angle between the fivefold vectors is about 63.4°. The fivefold zone axes in Cartesian coordinates are given as ⟨1 τ 0⟩ (the equivalent indices are generated by cycling, but not permutation). Perpendicular to fivefold axes occur another important zone axis ⟨τ 1 0⟩ in which a twofold and a fivefold vector are at 90° to each other [18]. This diffraction pattern is shown in Fig. 1d.

3.1. Relationship 1

Fig. 2a shows the [1 0 0] zone axis diffraction pattern from the φ-phase. In this pattern, {0 6 4} spots are high intensity spots. They are in fact the highest intensity spots in the reported powder diffraction pattern [15]. These {0 6 4} spots are observed to make a rectangle similar to a Golden rectangle in the twofold diffraction pattern of an icosahedral phase (as in Fig. 1a). Thus we assume that the {0 6 4} reciprocal vectors correspond to fivefold vectors of an icosahedral phase. Fig. 2b shows the [0 0 1] diffraction pattern. In this pattern there are many strong spots with similar intensities. However, {3 4 0} spots can be seen making a Golden rectangle. In the [0 1 0] pattern, Fig. 2c, a Golden rectangle can be defined by strong

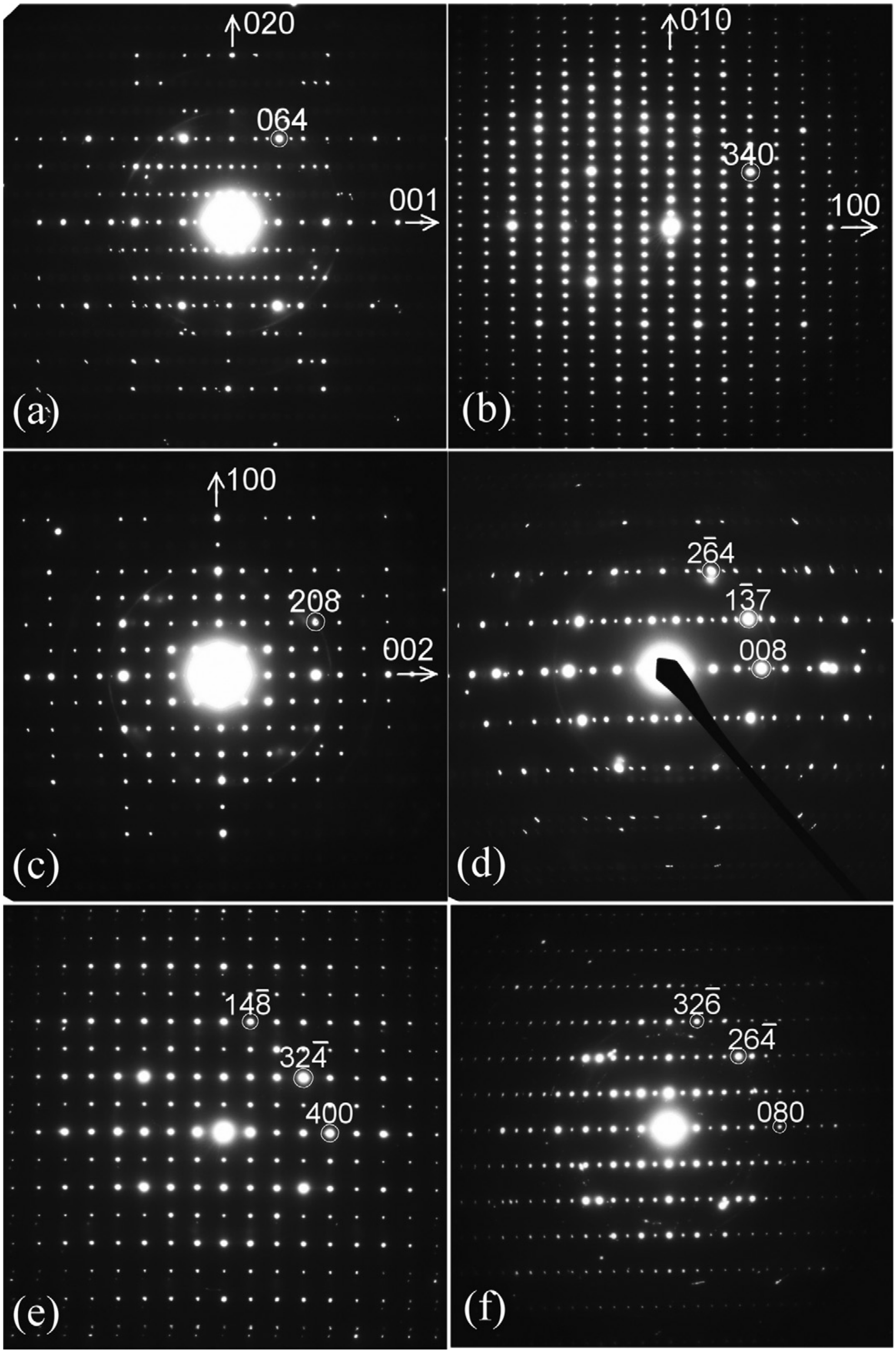

Fig. 2. Diffraction patterns from the φ-phase on which important diffraction spots relating it the icosahedral phase (by relationship 1) are marked. (a) [1 0 0], (b) [0 0 1], (c) [0 1 0], (d) [3 1 0], (e) [0 2 1] and (f) [2 0 1] zone axis diffraction patterns.

spots {2 0 8}. Thus {0 6 4}, {3 4 0} and {2 0 8} are identified as the six vectors corresponding to the six icosahedral fivefold vectors. With this information, a stereogram is drawn in Fig. 3, on which an icosahedral stereogram is superimposed. It is observed that the traces of fivefold vectors nearly coincide with the traces of the {0 6 4}, {3 4 0} and {2 0 8} planes. In this superimposition it is also observed that the fivefold axes correspond to [3 1 0], [0 2 1] and [3 0 2] axes. A near match of reciprocal vectors/planar traces also shows that {2 $\bar{6}$ 3}, {3 2 $\bar{4}$}, {2 $\bar{6}$ 4}, {1 $\bar{3}$ $\bar{7}$} and {1 $\bar{4}$ 8} correspond to icosahedral twofold vectors.

A diffraction pattern from the [3 1 0] zone axis is shown in Fig. 2d. A pseudo-fivefold symmetry made by strong spots is immediately

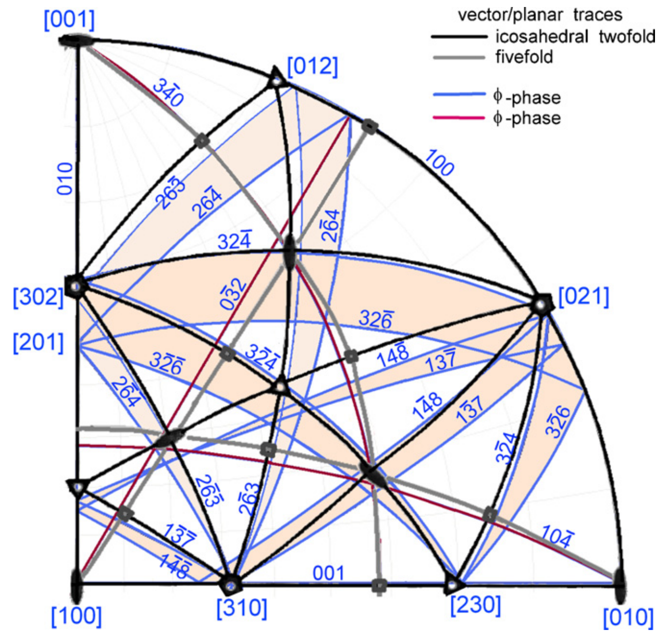

Fig. 3. A stereogram of the φ-phase overlaid with icosahedral phase stereogram showing relationship 1. Traces of φ-phase planes corresponding to icosahedral twofold and fivefold reciprocal vectors are drawn and marked with indices.

observed. From this, {2 $\bar{6}$ 4}, {1 $\bar{3}$ 7} and {0 0 8} are identified as pseudo-twofold vectors. Similarly, from the [0 2 1] diffraction pattern (Fig. 2e), {1 4 $\bar{8}$}, {3 2 $\bar{4}$} and {4 0 0} are identified as making a pseudo-fivefold symmetry, and that these vectors correspond to icosahedral twofold vectors. Tilting along the (0 1 0) vector, the [2 0 1] zone axis was found to resemble a pseudo-fivefold pattern more than the [3 0 2]. The [2 0 1] pattern is shown in Fig. 2f. In this pattern, {3 2 $\bar{6}$}, {2 6 $\bar{4}$} and {0 8 0} vectors are identified as pseudo-twofold, making a pseudo-fivefold symmetry.

In the transformation from a quasicrystal to a crystalline phase, splitting of zone axes and reciprocal vectors are observed. A fivefold axis may be considered to be split into [3 0 2] and [2 0 1] axes by the appearance. Similarly, a splitting of icosahedral twofold vectors in the φ phase is also observed. For example, in the [0 2 1] diffraction pattern the {3 2 $\bar{4}$} vector is identified to be a pseudo-twofold, but in [2 0 1] it is the {3 2 $\bar{6}$} vector. Such pairs of vectors are shown with a shading between them.

3.2. Relationship 2

One more correspondence between the φ phase and the icosahedral phase can be found, which will be referred to as relationship 2, as opposed to the relationship 1 described above. The [0 0 1] zone axis diffraction pattern also resembles a pseudo-fivefold pattern. As shown in Fig. 4a, strong intensity spots {4 0 0}, {3 4 0} and {1 7 0} make the pseudo-twofold vectors. Following this crystallographic relationship, a stereogram is plotted again in Fig. 5, superimposing an icosahedral stereogram on φ phase, such that the [0 0 1] axis now corresponds to a fivefold axis. The [0 1 0] zone axis, as shown in Fig. 4b, now corresponds to a ⟨τ 1 0⟩ zone axis in which a fivefold reciprocal vector occurs at 90° to a twofold vector (Fig. 1d). This explains a square-like appearance of the diffraction pattern. The {4 0 0} vector corresponds to an icosahedral twofold vector while {0 0 8} corresponds to a fivefold vector.

The zone axis [1 0 0] must still correspond to an icosahedral twofold axis but in a different manners than in the previous relationship. Now a {0 6 4} and the {0 0 8} spot correspond to fivefold and mimic a Golden rectangle (Fig. 4c). Twofold vectors are represented by {0 4 8} and another {0 $\bar{6}$ 4}, which make a 90° angle between them. The [0 2 1] pattern, Fig. 4d, remains a pseudo-fivefold pattern with {1 4 $\bar{8}$}, {3 2 $\bar{4}$} and {4 0 0} as pseudo-twofold vectors. Zone axis [1 2 0] pattern (Fig. 4e) can now be described as a pseudo-twofold pattern in which {0 0 $\bar{8}$} and {4 $\bar{2}$ $\bar{4}$} spots are pseudo-fivefold, while {2 $\bar{1}$ $\bar{7}$} and {4 $\bar{2}$ 4} correspond to twofold vectors. It is highly distorted – the {0 0 $\bar{8}$} and {4 $\bar{2}$ $\bar{4}$} vectors make 66.2° angle, and the rectangle is actually a parallelogram with 76° angle. The angle between {2 $\bar{1}$ $\bar{7}$} and {4 $\bar{2}$ 4} is 81°. Similarly, [3 1 0] diffraction (Fig. 4f) also corresponds to a twofold axis, with {0 0 8} and {2 $\bar{6}$ 4} as pseudo-fivefold vectors, and {1 $\bar{3}$ 7} and {2 $\bar{6}$ $\bar{4}$} corresponding to icosahedral twofold vectors. Here the angle between the {0 0 8} and {2 $\bar{6}$ 4} vectors is 64°, and between the {1 $\bar{3}$ 7} and {2 $\bar{6}$ $\bar{4}$} vectors is 86°.

Correspondences of vectors to icosahedral vectors in these two relationships are listed in Table 1.

Table 1
Correspondence of φ-phase plane normals to icosahedral reciprocal vectors. 2f and 5f represent twofold and fivefold icosahedral reciprocal vectors, respectively. The labels indicate the particular icosahedra (A, B or C) corresponding to each reflection, as illustrated in Fig. 6.

Spot	Relationship		Label
	OR1	OR2	
080	2f (1)	5f (1)	B, C
040	2f (1)		A
400	2f (1)	2f (1)	A
064	5f (2)	5f (1), 2f (1)	A(5f), C(5f)
340	5f (2)	2f (2)	C(2f), B(2f)
208	5f (2)	–	C(2f), B(2f)
264/263	2f (4)		A(2f), B(2f)
137/148	2f (4)		C(2f)
324/326	2f (4)		A(2f), B(5f)
170		2f (2)	A(90–2,5)
324		2f (2)	A(2f), B(5f)
424		5f (2)	A(2f), B(5f)
217		2f (2)	A(5f), B(2f)
137		2f (2)	C(2f)
264		2f (2)	C(5f), B(2f)
263		5f (2)	C(5f)
012		2f (1)	B(2f)

4. Discussion

Using Eq. (1) and assuming a_R to be 0.515 nm [13], the lattice parameters for 0/1, 1/0, 1/1 and 2/1 approximants can be calculated to be 0.541, 0.876, 1.417 and 2.294 nm, respectively. The *a*-lattice parameter of the φ-phase corresponds to the value of a 1/0 approximant. The other two lattice parameters do not come close to any of these calculated values. In case of relationship 2, three orthogonal axes can be chosen to correspond to icosahedral twofold axes close to [1 0 0], [0 $\bar{2}$ 1] and [0 2 3]. The pole coincident with the [0 2 3] axis is (0 1 2), whose interplanar spacing is 0.852 nm. The pole close to [0 $\bar{2}$ 1] is {0 3 2}, with interplanar spacing of 0.488 nm. Thus a new orthorhombic cell which is an approximant to the icosahedral phase can be defined as 0.90 nm × 0.85 nm × 0.49 nm, which is a 1/0 1/0 0/1 approximant.

Examples of crystalline phases which are closely related to quasicrystals but are not approximants are hexagonal phases found in Al–TM (where TM is a transition metal) and Zn–Mg–RE (where RE is a rare earth element) systems [19–21]. Singh et al. [22] showed that these phases contain a cluster of three icosahedra each with a twofold axis coincident with the hexagonal axis of the unit cell. Presence of such clusters, called I3 clusters, was shown by Kreiner and Franzen [23]. These phases show a definite ratio of hexagonal *c*/*a* ratio, and were shown to be Frank's 'cubic-hexagonal' phase [24,25].

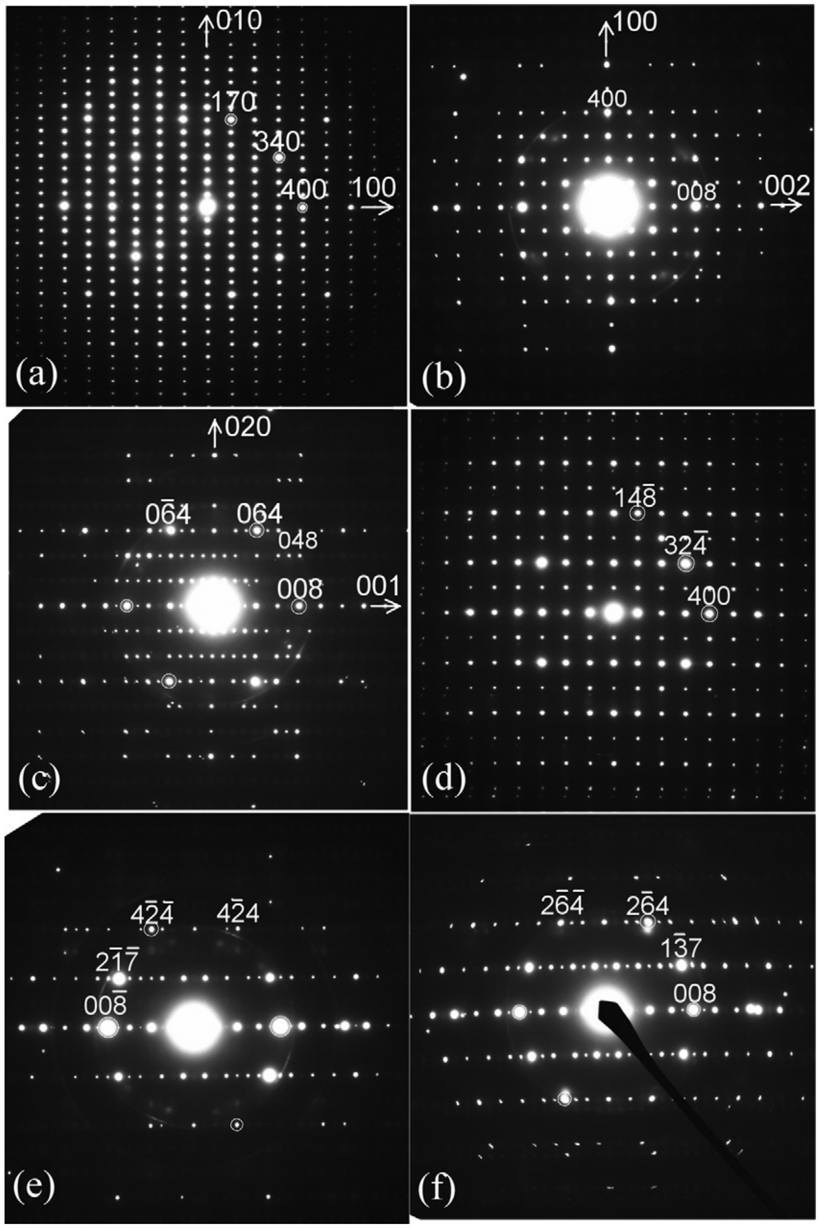

Fig. 4. Diffraction patterns from the φ-phase on which important diffraction spots relating it the icosahedral phase by relationship 2 are marked. (a) [0 0 1], (b) [0 1 0], (c) [1 0 0], (d) [0 2 1], (e) [1 2 0] and (f) [3 1 0] zone axis diffraction patterns.

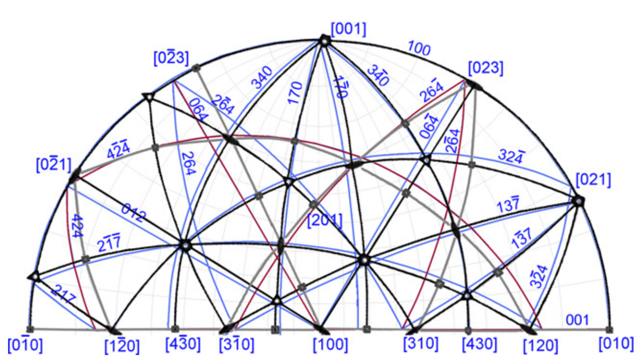

Fig. 5. A stereogram showing relationship 2 between the φ-phase and the icosahedral phase. Planar traces of the φ-phase corresponding to the icosahedral twofold and fivefold planes are drawn.

In both relationships 1 and 2, a commonality is the coincidence of an icosahedral twofold axis with [1 0 0]. To go from relationship 1 to 2, a rotation of 58.3° is made about this axis. This rotation can be made in two directions. Thus a total of three orientations of icosahedra exist about this twofold axis. This is similar to the case of the Frank's cubic-hexagonal phases. In these hexagonal phases, zone axes $\langle 1\ 1\ \bar{2}\ 0\rangle$ correspond to an icosahedral twofold as well as a fivefold. Similar is the case for the corresponding [0 0 1] zone in the φ-phase (Figs. 2b and 4a). An analogous zone axis is ⟨0 2 1⟩, in which again a twofold and a fivefold correspondence is observed (in relationship 1, both variants of ⟨0 2 1⟩ identically correspond to fivefold; in relationship 2, one ([0 2 1]) corresponds to a fivefold while the other ($\left[0\ \bar{2}\ 1\right]$) corresponds to an icosahedral twofold axis (Fig. 5). In a Frank's hexagonal phase the zone $\langle 1\ 0\ \bar{1}\ 0\rangle$ corresponds to the icosahedral $\langle \tau\ 1\ 0\rangle$ (common for two orientations of icosahedra). The same appearance is observed very clearly along the [0 1 0] zone axis, as noted above. The ⟨0 2 3⟩ axis is at about 60° from [0 1 0] (around [1 0 0] axis). The ⟨0 2 3⟩

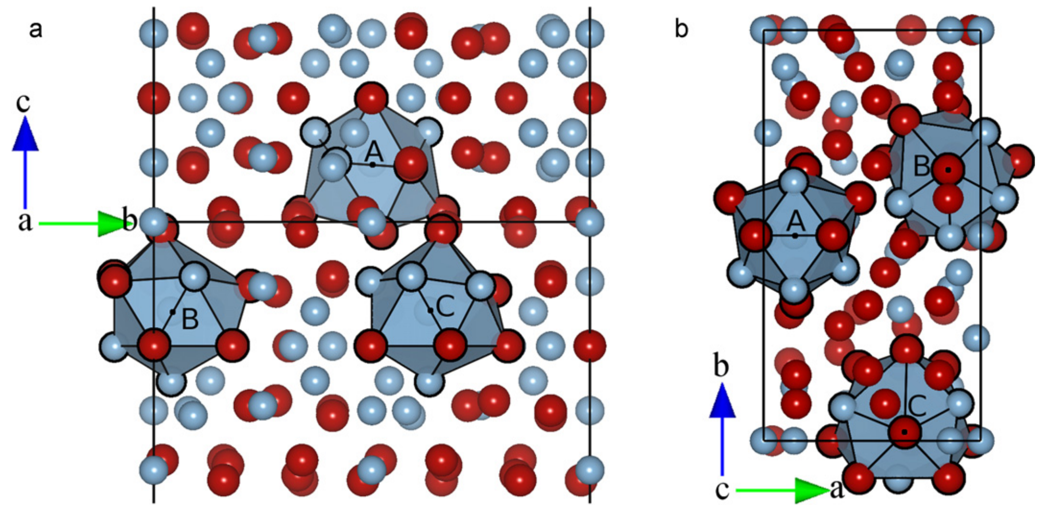

Fig. 6. Schematics of the φ-phase unit cells viewed along the (a) [1 0 0] and (b) [0 0 1] axes. Three differently oriented icosahedral clusters (A, B and C) are shown. Icosahedron A has a cube orientation with twofold axes parallel to [1 0 0], [0 1 0] and [0 0 1] directions. Icosahedra B and C have twofold axes parallel to [0 1 0] and a five-fold axis along [0 0 1]. The relationships between icosahedra and the φ-phase planes are set out in Table 1.

zone axis diffraction pattern also shows a square-like appearance in its intensity, characteristic of a ⟨τ 1 0⟩ zone axis pattern. The φ-phase axis [1 0 0] must then correspond to a hexagonal axis of a Frank's hexagonal phase. This correspondence is brought out by the intense spots {0 6 4} and {0 0 8}, which make a hexagonal arrangement. The angle between them is almost 60°, and both have close interplanar spacings of about 0.24 nm. It must be mentioned again that the spots {0 6 4} have the highest intensity and the {0 0 8} spot is one of the highest intensity spots in this structure. Thus we can approximate the unit cell of the φ-phase with a hexagonal cell with *c* parameter as 1.97 nm. The *a* lattice parameter can be calculated from spots {0 2 1} or (0 0 3), whose interplanar spacings are 0.777 and 0.657 nm, respectively. These give the *a* lattice parameter to be 0.897 nm or 0.657 nm. Thus the *c*/*a* ratio can be calculated to be from 1.1 to 1.3. These match well with the *c*/*a* ratio for a cubic-hexagonal phase, which is $(3/2)^{1/2} = 1.22$ [24,25].

Verification of these icosahedral coordinations can be observed in the structure of the φ-phase proposed by Bourgeois et al. [16]. Fig. 6 shows the structure of the φ-phase along *a* [1 0 0] and *c* [0 0 1] axes. Icosahedra in three orientations A, B and C can be defined. All are oriented with a twofold axis along the *a*-axis (Fig. 6a). Along the *c* axis, icosahedron A is oriented along a twofold axis, while B and C are oriented nearly along fivefold axes. Distortions in the icosahedra are observed due to differences in the atomic radii. The correspondences between the φ-phase diffraction spots and the two-fold and five-fold vectors of icosahedra A, B and C are set out in Table 1.

5. Conclusions

An electron diffraction study of the orthorhombic φ-$Al_5Mg_{11}Zn_4$ phase shows that, although it is not strictly an approximant phase, it is closely related to quasicrystalline phases. Its unit cell structure contains icosahedra in three orientations. One icosahedral orientation has a set of three mutually perpendicular twofold axes oriented along ⟨1 0 0⟩ axes of the unit cell and a fivefold axis along [3 1 0]. Two other icosahedra are oriented with a fivefold axis along [0 0 1] axis and a twofold axis along [1 0 0]. Therefore this phase is similar to hexagonal phases in Al–TM (TM = transition metal) and Zn–Mg–RE (RE = rare earth element) alloys, that are closely related to the quasicrystalline phases. However, due to distortions of the icosahedra, the unit cell here is orthorhombic instead of hexagonal.

References

[1] I.J. Polmear, Mater. Sci. Technol. 10 (1984) 1.
[2] G. Bergman, J.L.T. Waugh, L. Pauling, Acta Cryst. 10 (1957) 254.
[3] K.N. Ishihara, Mater. Sci. Forum 22–24 (1986) 223.
[4] D. Gratias, J.W. Cahn, Scripta Metall. 20 (1986) 1193.
[5] N.K. Mukhopadhyay, K.N. Ishihara, S. Ranganathan, K. Chattopadhyay, Acta Metall. Mater. 39 (1991) 1151.
[6] M. Cooper, K. Robinson, Acta Cryst. 20 (1966) 614.
[7] V. Elser, C.L. Henley, Phys. Rev. Lett. 55 (1985) 2883.
[8] P. Guyot, M. Audier, Phil. Mag. A52 (1985) L15.
[9] M. Audier, S. Sainfort, B. Dubost, Phil. Mag. A54 (1986) L105.
[10] C.L. Henley, V. Elser, Phil. Mag. A53 (1986) L43.
[11] K. Knowles, in: Ch. Janot, J.M. Dubois (Eds.), Quasicrystalline Materials, World Scientific, Singapore, 1988.
[12] T. Rajasekharan, D. Akhtar, R. Gopalan, K. Muraleedharan, Nature 322 (1986) 528.
[13] W.A. Cassada, Y. Shen, S.J. Poon, G.J. Shiflet, Phys. Rev. B 34 (1986) 7413.
[14] L. Bourgeois, C.L. Mendis, B.C. Muddle, J.F. Nie, Philos. Mag. Lett. 81 (2001) 709.
[15] P. Donnadieu, A. Quivy, T. Tarfa, P. Ochin, A. Dezellus, M.G. Harmelin, P. Liang, H.L. Lukas, H.J. Seifert, F. Aldinger, G. Effenberg, Z. Metallkd. 88 (1972) 12.
[16] L. Bourgeois, B.C. Muddle, J.F. Nie, Acta Mater. 49 (2001) 2701.
[17] V. Elser, Phys. Rev. B 32 (1985) 4892.
[18] K. Chattopadhyay, S. Lele, R. Prasad, S. Ranganathan, G.N. Subbanna, N. Thangaraj, Scripta Metall. 19 (1985) 1331.
[19] L.A. Bendersky, J. Microsc. 146 (Pt. 3) (1987) 303.
[20] K.Y. Wen, Y.L. Chen, K.H. Kuo, Metall. Trans. 23A (1992) 2437.
[21] E. Abe, H. Takakura, A. Singh, A.P. Tsai, J. Alloys Compd. 283 (1998) 169.
[22] A. Singh, E. Abe, A.P. Tsai, Phil. Mag. Lett. 77 (2) (1998) 95.
[23] G. Kreiner, H.F. Franzen, J. Alloys Compd. 261 (1997) 83.
[24] F.C. Frank, Acta. Cryst. 18 (1965) 862.
[25] S. Ranganathan, A. Singh, A.P. Tsai, Phil. Mag. Lett. 82 (2002) 13.